Copyright Notice:

©2005 Wang Electro-Opto Corporation. Personal use of this material is permitted. However, reprinting/republishing of this material or reuse of any copyrighted component of this work in other works is disallowed.

Theory of a Class of Planar Frequency-Independent Omnidirectional Traveling-Wave Antennas

Johnson J. H. Wang
Wang Electro-Opto Corporation (WEO)
Marietta, Georgia 30067 USA
Email: jjhwang@weo.com

I. Introduction

There is a growing interest in ultra-wideband (UWB) antennas due to expanding applications in wireless communications, networking, detection, sensing, etc. Although UWB is defined by IEEE as having a fractional bandwidth wider than 20%, to many UWB means "DC to daylight." In this context the frequency-independent (FI) traveling-wave (TW) antenna is an ideal candidate. For many practical applications the antenna must have an omnidirectional pattern, and be planar in shape with low-profile and platform-conformable features.

Recently, such an antenna with a 10:1 gain bandwidth (1-10 GHz) was reported [1]. It was a mode-0 SMM (spiral-mode microstrip) antenna 5.7-inch in diameter and 1.06-inch in height [2]. The general theory for this antenna as a TW antenna has been developed, and its solution by the method of stationary phase discussed in [3, 4]. This paper presents details on this theory for the omnidirectional type (the mode-0).

II. Formulation of a Planar FI Omnidirectional TW Antenna

The new class of FI omnidirectional TW antenna is depicted in Fig. 1.

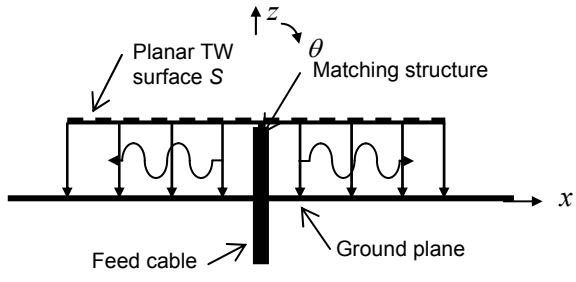

Figure 1. Mode-0 SMM antenna in transmit operation.

The planar broadband TW surface S can be a multiarm spiral, and is of a finite and preferably small diameter. The ground plane also has a finite diameter dictated by the mounting platform. Both planar structures are conformal to the surface of the platform. The use of spherical, cylindrical and rectangular systems with (r, θ, ϕ), (ρ, ϕ, z) and (x, y, z) coordinates, respectively, is implicit, with the z-axis being normal to the ground plane.

Without loss of generality, and in light of the reciprocity theorem, we consider only the transmit case. It is assumed that a TW wave, specifically a mode-0 SMM wave [2], has been successfully launched. The mode-0 SMM wave corresponds to the case with spiral mode number $n = 0$, in which all the spiral arms are excited in equal amplitude and phase. It is assumed that a traveling wave is largely supported and confined between the planar broadband structure and the ground plane.

The far-zone radiation can be readily derived from a simple TW theory in closed form since the source and fields are sufficiently decoupled. We will formulate the problem in terms of a magnetic current $\boldsymbol{M}$ over the nonconducting part of the antenna surface, S, which is the slot region, instead of an equivalent electrical current for other FI antennas of non-zero modes [4].

By the image theory, the magnetic field in the far zone due to $\boldsymbol{M}$ with the conducting surface removed is

$$\boldsymbol{H(r)} = \frac{-jke^{-jkr}}{4\pi\eta r}\int_S 2\boldsymbol{M}(\boldsymbol{r'})e^{jk\hat{r}\cdot\boldsymbol{r'}}ds' \qquad (1)$$

where $k = 2\pi/\lambda$, λ is the wavelength of the TW, and η is the free-space wave impedance equal to $\sqrt{\mu_o/\varepsilon_o}$ or 120π. The primed and unprimed position vectors and coordinates refer to source and field points, respectively. The equivalent magnetic current $\boldsymbol{M}$ is given by

$$\boldsymbol{M} = -\hat{z}\times\boldsymbol{E} \qquad \text{over the slot region } \boldsymbol{r}' \qquad (2)$$

The integral in Eq. (1) can be evaluated as a Riemann-Stieltjes integral by noting that

$$\iint_S \boldsymbol{f}(\boldsymbol{r};\rho',\phi')\rho' d\rho' d\phi' = \sum_{\ell=1}^{\ell=N}\boldsymbol{F}_\ell(\theta,\phi)S_\ell \qquad (3)$$

where $\boldsymbol{f}$ denotes an arbitrary but integrable function, and we define

$$S_\ell \equiv \int_{\rho_\ell}^{\rho_{\ell+1}} g(\boldsymbol{r};\rho')\,d\rho' \tag{4}$$

S_ℓ in Eq. (4) is proportional to the far-zone radiated field of the well-known thin circular annular slot with uniform aperture excitation. This is both physically and mathematically significant, and we will take advantage of this relevance by examining the annular slot first.

III. The Annular Slot Antenna as a Building Block

Fig. 2 depicts a thin circular annular slot on a ground plane in the x-y plane, which is a building block of this theory. The thin circular slot has a mean radius a, excited by a uniform radial electric field parallel to ρ, with a resulting voltage V across the slot aperture.

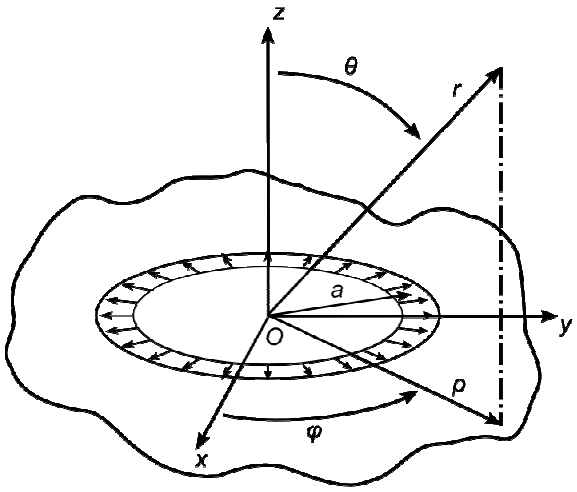

Fig. 2. A thin annular slot on x-y plane.

It can be shown that the far-zone radiation of this annular slot is fully represented by a magnetic field having only a ϕ component as follows:

$$H_\phi(\phi) = \frac{jaV\exp(-jkr)}{120\pi\lambda r}\int_0^{2\pi}\cos(\phi-\phi')\exp[jka\sin\theta\cos(\phi-\phi')]\,d\phi' \tag{5}$$

The integral in Eq. (5) can be evaluated exactly as

$$H_\phi = \frac{-aV\exp(-jkr)}{60\lambda r}J_1(ka\sin\theta) \tag{6}$$

where J_1 denotes a Bessel function of the first kind of order 1. For a small slot ($a \le \lambda/(2\pi)$), we have

$$H_\phi \cong \frac{-V\exp(-jkr)}{60r}\frac{A}{\lambda^2}\sin\theta \quad \text{as } a \to 0 \tag{7}$$

where $A = \pi a^2$.

To our knowledge these equations have appeared only in [5, 6], but with some errors. We believe references 5 and 6 are in error since Eq. (6) can be verified independently by invoking duality from the case of an electric circular loop antenna based on Maxwell equations having full-fledged presentation of magnetic sources [7].

Other errors in annular slots in the 1st edition of the widely used antenna handbook [5] include Figs. 8-11 (b) and 27-43, which were largely eliminated in its 3rd edition. Corrections for these are also long overdue.

An electrically small annular slot has a desired elevation pattern, sin θ, according to Eq. (7). However, the beam becomes tilted and narrowed, with additional beams emerging, as the frequency increases. Thus, its usefulness as a wideband omnidirectional antenna is limited.

Fig. 3 shows the calculated angle of the elevation beam peak as a function of ka using Eq. (6). (Only two beams are included in Fig. 3.) As can be seen, for annular slots of a small diameter a, the pattern is simply sin θ as given by Eq. (7), peaked at $\theta = 90^o$, which is ideal for omnidirectional coverage.

Note that around $ka = 2$ the first beam tilts up rapidly as ka increases. It is also worth mentioning that omnidirectional antennas, such as a monopole or annular slots, mounted on a finite ground plane of radius b have an increasing beam tilt in elevation as kb decreases. These two beam tilt mechanisms were misleadingly presented in Fig. 27-43 in the 1st ed. of [5].

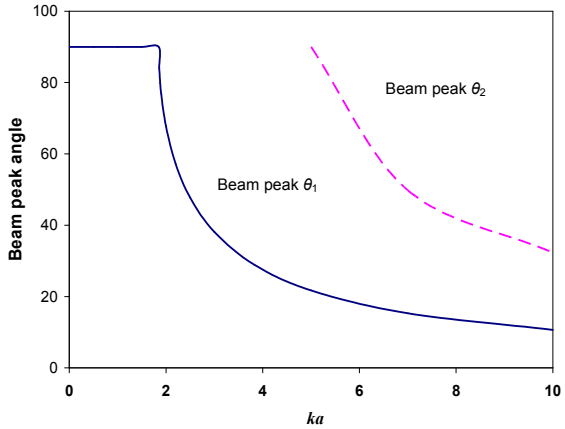

Fig. 3. Beam peaks versus ka for an annular slot.

IV. The TW Antenna as an Array of Annular Slots Plus Edge Slot

Based on the discussions above, the far-zone radiated fields of the planar FI omnidirectional antenna in Fig. 1 is given by

$$H = H_\phi = \sum_{\ell=1}^{\ell=N} H_\ell(\theta,\phi) = \sum_{\ell=1}^{\ell=N} \frac{-a_\ell V_\ell \exp(-jkr)}{60\lambda r} J_1(ka_\ell \sin\theta) e^{j\psi_\ell} \quad (8)$$

where ψ_ℓ and V_ℓ denote, respectively, the phase and amplitude of the voltage of the equivalent annular slot element ℓ. Thus the far-zone radiation of the TW surface S can be fully represented by its magnetic field, which only consists of a ϕ component, and which is the superposition of the fields from the concentric annular slots of varying amplitude and phase, V_ℓ and ψ_ℓ, respectively, along ρ.

Therefore, the far-zone radiated field of this TW antenna is the superposition of the fields due to the elements of a concentric array of equally spaced annular slots, plus a circular edge slot at the rim of the spiral.

V. Radiation Zones and Radiated Fields

Consider the case in which the planar structure in Fig. 1 is a self-complementary 2-arm Archimedean spiral. The center lines of a two-arm Archimedean spiral on the S plane are

$$\rho_1 = b\phi \qquad \phi \varepsilon [\phi_0,\ \phi_t] \quad (9a)$$

$$\rho_2 = b(\phi - \pi) \qquad \phi \varepsilon [\phi_0 + \pi,\ \phi_t + \pi] \quad (9b)$$

The two feed points are at $\phi = \phi_0$ and $(\phi_0 + \pi)$ for arms #1 and #2, respectively, with equal in-phase voltages V.

The arc lengths L_1 along spiral arm #1 from its feed point to $(\rho,\ \phi)$, and L_2 along the adjacent spiral arm #2 from its feed point to $(\rho_2,\ \phi)$, respectively, are given by

$$L_1 = \frac{b}{2}\left[\phi\sqrt{1+\phi^2} + \sinh^{-1}\phi\right]_{\phi_0}^{\phi} \quad (10a)$$

$$L_2 = \frac{b}{2}\left[\phi\sqrt{1+\phi^2} + \sinh^{-1}\phi\right]_{\phi_0}^{\phi-\pi} \quad (10b)$$

Also, between adjacent arms,

$$\Delta\rho \equiv b\phi - b(\phi - \pi/2) = b\pi/2 \quad (11a)$$

$$\Delta L \equiv (L_1 - L_2) \sim \rho\Delta\rho/b \sim \pi\rho \quad \text{as } |a| \to 0 \quad (11b)$$

The phase change $\Delta\psi_J$ of the TW fields between adjacent spiral arms is given by

$$\Delta\psi_J = (2\pi/\lambda)\Delta L \quad (12)$$

The series in Eq. (8) can be approximately evaluated by including only a few terms that have significant in-phase contribution. Physically, this means including only slots at the "radiation zones." For a 2-arm spiral, the radiation zones are at circumferences where $\Delta\psi_J = \pi/2$ between adjacent arms, so that an equivalent annular slot is formed over three adjacent arms (or two adjacent annular slots), with a resulting voltage V. For a 4-arm spiral, at radiation zones $\Delta\psi_J = \pi/4$ between five adjacent arms or four adjacent slots. Thus, radiation zones are at radial distances ρ_r given by

$$\rho_r = \lambda/(4\pi) + n\lambda/\pi \qquad \text{for 2-arm spiral} \quad (13a)$$

$$\rho_r = \lambda/(8\pi) + n\lambda/\pi \qquad \text{for 4-arm spiral} \quad (13b)$$

where $n = 0, 1, 2, 3\ldots$, and the edge of the spiral.

Fig. 4 shows measured elevation patterns for a 4-arm mode-0 SMM antenna of Fig. 1, 5.7-inch in diameter and 1.06-inch in height operating over 0.5-10 GHz, described in [1]. As can be seen, the patterns are consistent with Eq. (8) and Fig. 3 with regard to the beam tilt and beam peaks as a/λ increases from 0.12 to 2.42 (or ka from 0.75 to 15.08). For example, at 2.5 GHz, ka = 3.75, the beam peaked at $\theta \sim 42^o$ can be calculated from two terms in Eq. (8)—the fields from two radiation zones n = 1, 2 in Eq. (13b).

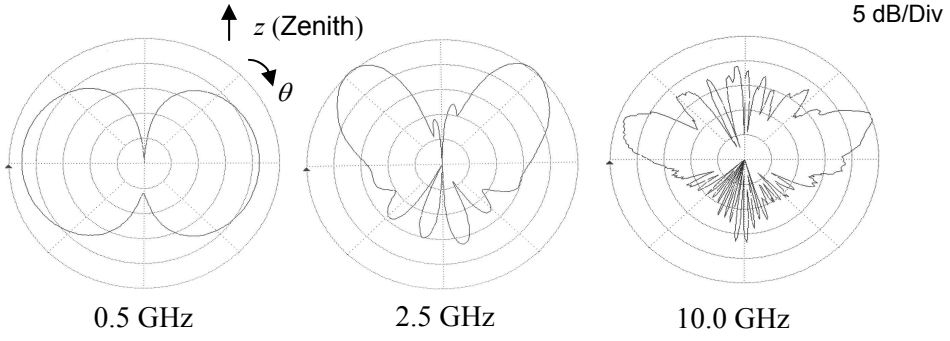

Fig. 4. Measured elevation patterns.

VI. Impedance Matching

Under the condition that higher-order modes are suppressed, the planar TW surface S can be considered a loaded surface consisting of both a reactive component and a resistive component, the latter accounting for possible radiation through the nonconducting (slot) region. At the edge of the surface S, there is a circular slot from which the residual power is radiated.

In the region where the planar surface structure S is a solid conductor, the TW antenna can be viewed as a circular radial waveguide of height h, and its characteristic impedance Z_{00} at ρ for the $m = n = 0$ mode is given by

$$Z_{00} = 60h/\rho \tag{14}$$

Note that Z_{00} changes with ρ, the distance from the center of the radial waveguide, but is independent of frequency.

In regions where the surface S is self-complementary, half metallic and half slot, its characteristic impedance Z_c can be obtained, by invoking the principle of superposition and duality in the context of Maxwell equations formulated with full-fledged presentation of magnetic sources [7], as

$$Z_c \sim 2\, Z_{00} \tag{15}$$

Each annular slot can be represented by a radiation resistance plus a small capacitance. Various techniques are available to suppress higher-order modes to ensure that the simple transmission line model is an adequate representation for the radial waveguide with generally reactive TW surface S.

Eqs. (14) and (15) are consistent with our experimental observations. Indeed, ultra-wideband impedance matching over 10:1 bandwidth has been demonstrated, with SWR < 1.3 mostly, rising to ~ 2.0 at high and low frequencies, over a 10:1 bandwidth (at 1-10 GHz and other frequency ranges) with breadboard and brassboard models. Some of the results have been presented in [1].

It is worth commenting that the self-complementary geometry of the TW surface S, the frequency-independent impedance of Z_{00}, and the full-fledged duality formulation of the Maxwell equations, all contributed to the insight that ultra-wideband impedance matching for the planar FI TW antenna in Fig. 1 is feasible.

VII. Conclusions

The theory for a new class of planar frequency-independent omnidirectional antenna has been developed and found to be consistent with measured data, with better agreement than many of those obtained by brute-force numerical computation. More importantly, the theory is useful for design and synthesis because of its simple closed-form solution, which has direct and close relevance to the physical parameters and performance of the planar frequency-independent omnidirectional antenna. A building block for the theory is that for the annular slots, which has some errors in the literature. These errors in the equations and figures were also discussed and corrected in this paper.

References

1. J. J. H. Wang, C. J. Stevens, and D. J. Triplett, "Ultrawideband Omnidirectional Conformable Low-Profile Mode-0 Spiral-Mode Microstrip (SMM) Antenna," 2005 *IEEE Antennas and Prop. Symp*., Washington, DC, July 2005.
2. J. J. H. Wang, "The Spiral as a Traveling Wave Structure for Broadband Antenna Applications," *Electromagnetics*, 20-40, July-August 2000; also U.S. Patents #5,508,710, April 16, 1996, and #5,621,422, April 15, 1997.
3. J. J. H. Wang, "The Physical Foundation, Developmental History, and Ultra-wideband Performance of SMM (Spiral-Mode Microstrip) Antennas," 2005 *IEEE Antennas and Prop. Symp*., Washington, DC, July 2005.
4. J. J. H. Wang, "Theory of Frequency-Independent Antennas as Traveling-Wave Antennas and Their Asymptotic Solution by Method of Stationary Phase," *2005 International Symposium on Antennas and Propagation (ISAP)*, Seoul, Korea, August 3-5, 2005.
5. H. Jasik, editor; *Antenna Engineering Handbook*, McGraw-Hill, New York, 1st ed., 1961; also 3rd edition, R. C. Johnson, editor, 1993.
6. A. A. Pistolkors, "Theory of the Circular Diffraction Antenna," *Proc. IRE*, pp. 56-60, January 1948.
7. J. J. H. Wang, *Generalized Moment Methods in Electromagnetics — Formulation and Computer Solution of Integral Equations*, pp. 6-7, 105-107, Wiley, New York, 1991.